

PUBLISHED VERSION

Nishimura, A.; Mitsui, Go; Nakamura, Katsuya; Hirota, M.; Hu, Eric Jing
CO₂ reforming characteristics under visible light response of Cr- or Ag-doped TiO₂ prepared by sol-gel and dip-coating process, *International Journal of Photoenergy*, 2012; 2012:Article ID 184169.

Copyright © 2012 Akira Nishimura et al.

This is an open access article distributed under the [Creative Commons Attribution License](#), which permits unrestricted use, distribution, and reproduction in any medium, provided the original work is properly cited.

PERMISSIONS

<http://www.hindawi.com/journals/ijp/guidelines/>

Open Access authors retain the copyrights of their papers, and all open access articles are distributed under the terms of the Creative Commons Attribution license, which permits unrestricted use, distribution and reproduction in any medium, provided that the original work is properly cited.

2nd December 2013

<http://hdl.handle.net/2440/70262>

Research Article

CO₂ Reforming Characteristics under Visible Light Response of Cr- or Ag-Doped TiO₂ Prepared by Sol-Gel and Dip-Coating Process

Akira Nishimura,¹ Go Mitsui,¹ Katsuya Nakamura,¹ Masafumi Hirota,¹ and Eric Hu²

¹ Division of Mechanical Engineering, Graduate School of Engineering, Mie University, 1577 Kurimamachiya-cho, Tsu 514-8507, Japan

² School of Mechanical Engineering, The University of Adelaide, Adelaide, SA 5005, Australia

Correspondence should be addressed to Akira Nishimura, nishimura@mach.mie-u.ac.jp

Received 25 May 2011; Revised 2 August 2011; Accepted 2 August 2011

Academic Editor: Jinlong Zhang

Copyright © 2012 Akira Nishimura et al. This is an open access article distributed under the Creative Commons Attribution License, which permits unrestricted use, distribution, and reproduction in any medium, provided the original work is properly cited.

A Cr- or Ag-doped TiO₂ film was prepared by sol-gel and dip-coating process and used as the photocatalyst for CO₂ reforming under the visible light. The ratio of amount of Cr or Ag added to amount of Ti in TiO₂ sol solution (R) varied from 0 to 100 wt% or 0 to 50 wt%, respectively. The total layer number of Cr- or Ag-doped TiO₂ film (N) coated was changed. The CO₂ reforming performance with the Cr- or Ag-doped TiO₂ film was tested under a Xe lamp with or without ultraviolet (UV) light. As a result, when N equals to 1, the concentration of CO which was a product from CO₂ reforming was maximized in Cr doping case for $R = 70$ wt% and in Ag doping case for $R = 1$ wt%, respectively. The best result of concentration of CO = 8306 ppmV, concentration of CH₄ = 1367 ppmV, concentration of C₂H₆ = 1712 ppmV is obtained when $N_{\text{top}} = 7$ with Cr doping in this study.

1. Introduction

Due to mass consumption of fossil fuels, global warming and fossil fuels depletion have become a serious global environmental problem in the world. After the industrial revolution, the averaged concentration of CO₂ in the world has been increased from 280 ppmV to 387 ppmV by 2009. Therefore, it is necessary to develop a new energy production technology with less or no CO₂ emission.

It is reported that CO₂ can be reformed into fuels, for example, CO, CH₄, CH₃OH and H₂, and so forth, by using TiO₂ as the photocatalyst under ultraviolet (UV) light illumination [1–10]. If this technique could be applied practically, a carbon circulation system would then be established: CO₂ from the combustion of fuel is reformed, using solar energy, to fuels again, and true zero emission can be achieved. Many R&D works on this technology have been carried out, using TiO₂ particles loaded with Cu, Pd, Pt to react with CO₂ dissolved in solution [1, 5, 7, 11–17]. Recently, nano-scaled TiO₂ [18–20], porous TiO₂ [21], TiO₂ film combined with

metal [22, 23], and dye-sensitized TiO₂ [24] are developed for this process. However, the fuel concentration in the products achieved in all the attempts so far is still low, ranging from 10 ppmV to 1000 ppmV, to be practically useful [1, 4, 5, 7, 8, 11, 12, 15, 16, 18, 20]. Therefore, the big breakthrough in increasing the concentration level is necessary to advance the CO₂ reforming technology.

In the applications such as water splitting and purification of pollutant, the photoresponse extension of TiO₂ to the visible spectrum has been investigated well [25–29]. TiO₂ by itself can only work under UV light due to its wide bandgap of 3.0–3.2 eV, which means that only about 4% of the incoming solar energy on the surface can be utilized [30]. On the other hand, the visible light accounts for 43% of whole solar energy [31]. Therefore, if the photoresponse of TiO₂ could be extended to the visible spectrum, the CO₂ reforming performance of TiO₂ technology would be improved significantly.

Doping with foreign ions is one of the most promising strategies for sensitizing TiO₂ to visible light and also for

forming charge traps to keep electron-hole pairs separate [32]. The most popular dopants for modification of the optical and photoelectrochemical properties of TiO₂ are transition metals such as Cr, Fe, Ni, V, Mn, and Cu [28]. Choi et al. [33] carried out a systematic investigation of the photocatalytic activity of TiO₂ doped with 21 different metal ions. It was found that doping with metal ions would introduce additional energy levels in the band gap of TiO₂ thus extending the photoresponse of TiO₂ into the visible spectrum. In addition, an optimum concentration of dopant metal ions exists under specific conditions. If the concentration of dopant exceeds the optimum one, the photocatalytic activity declines because of charge recombination [28]. Many previous reports on metal-doped TiO₂ used for photocatalytic degradation reaction of chemicals under visible light showed the activity enhancement only for a specific amount of doping ions, otherwise detrimental effects occur [34].

Many different techniques have previously been reported for metal doping of TiO₂ such as wet impregnation [35], hydrothermal deposition [36], RF magnetron sputtering deposition [24, 26, 37, 38], flame reactor method [39], solidstate reactions [40], ion implantation [41], and pulsed laser deposition [42]. Recently, the sol-gel method is adopted for metal doping of TiO₂ well [27–29, 34, 43–46] since this method can incorporate dopants into TiO₂ lattice, resulting in preparation of the materials with other optical and also catalytic properties [47]. In addition, the integration of dopants into the sol during the gelation process facilitates direct interaction with TiO₂ by sol-gel method [46].

Although many studies to extend the photoresponse of TiO₂ to the visible spectrum were reported as described above, there are only a few reports on its application for promoting the CO₂ reforming purposes [24]. In our previous studies [48–51], the effect of TiO₂ thin film preparation conditions in sol-gel and dip-coating process on the CO₂ reforming performance under UV light was investigated.

In this study, TiO₂ sol-gel and dip-coating process with doping is also adopted in order to extend its photoresponse to the visible spectrum to promote the CO₂ reforming performance. It was reported that the transition metals such as V, Cr, Mn, Fe, and Ni were effective for the photoresponse extension of TiO₂ to the visible spectrum [37]. According to the previous reports [28, 34, 39–41, 52, 53], it can be thought that Cr³⁺ or Cr⁶⁺ ion existing in TiO₂ film after doping can absorb the light of wavelength from 400 nm to 550 nm [28, 34, 39, 41, 52–55]. Therefore, Cr was selected at first as the dopant to check the feasibility of promoting CO₂ reforming performance of TiO₂ in this study. According to the study which investigated the photocatalytic H₂ evolution from water-alcohol mixtures, noble and base materials, including Pt, Au, Pd, Ni, Cu, and Ag, have been reported to be very efficient for increasing the production of H₂ by TiO₂ photocatalytic reaction [56]. According to the reaction scheme [1, 5, 6, 11, 16, 50, 51] of CO₂ reforming by TiO₂ photocatalyst as shown in Figure 1, if a lot of H⁺ is produced, the reduction process is promoted, resulting in increase of the concentration of produced fuel. In addition, the photoresponse extension of TiO₂ to the visible spectrum

was obtained by Ni, Cu, and Ag doping in the previous study on the photocatalytic H₂ evolution from water-alcohol mixtures [56]. TiO₂ doped with Ag⁺ ions absorbs the light of wavelength from 460 nm to 477 nm [56, 57]. Therefore, Ag was also selected at first as the dopant to check the feasibility of promoting CO₂ reforming performance of TiO₂ in this study.

In the present paper, the preparation method for doping Cr or Ag into TiO₂ film was developed. The characterization analyzed by scanning electron microscope (SEM), electron probe micro analyzer (EPMA), and X-ray photoelectron spectroscopy (XPS) was conducted. The influence of the ratio of amount of added Cr or Ag to amount of Ti in TiO₂ sol solution (*R*) and of the total coating number of Cr- or Ag-doped TiO₂ film (*N*) on CO₂ reforming characteristics under the condition of illuminating Xe lamp with or without UV light was also investigated in this study.

2. Experiment

2.1. Preparation of Cr- or Ag-Doped TiO₂ Film. Sol-gel and dip-coating process was used for preparing Cr- or Ag-doped TiO₂ film in this study. TiO₂ sol solution was made by mixing [(CH₃)₂CHO]₄Ti (purity of 95 wt%, Nacalai Tesque Co.) of 0.1 mol, anhydrous C₂H₅OH (purity of 99.5 wt%, Nacalai Tesque Co.) of 0.8 mol, distilled water of 0.1 mol, and HCl (purity of 35 wt%, Nacalai Tesque Co.) of 0.008 mol. Cr powders (08819-15, Nacalai Tesque Co., particle size below 74 μm) or Ag powders (30934-92, Nacalai Tesque Co., particle size below 44 μm) were added into TiO₂ sol solution. Copper disc whose diameter and thickness were 50 mm and 1 mm, respectively, was dipped into Cr/TiO₂ or Ag/TiO₂ sol solution and pulled up at the fixed speed (*RS*) of 0.22 mm/s. Then, it was dried out and fired under the controlled firing temperature (*FT*) and firing duration time (*FD*), resulting in the fact that Cr- or Ag-doped TiO₂ film was fastened on the surface of copper disc. *FT* and *FD* was set at 623 K and 180 s, respectively. In this study, *N* varied from 1 to 7 for Cr doping and from 1 to 5 for Ag doping.

2.2. Characterization of Cr- or Ag-Doped TiO₂ Film. The surface structure and crystallization characteristics of Cr- or Ag-doped TiO₂ film were evaluated by SEM (JXA8900R, JEOL Ltd.) and EPMA (JXA8900R, JEOL Ltd.). The EPMA analysis helps us not only to understand the coating state of Cr- or Ag-doped TiO₂ on copper disc but also to measure the amount of doped Cr or Ag within TiO₂ film on copper disc. Element distribution through thickness direction of Cr-doped TiO₂ film was analysed by XPS (PHI Quantera SXM, ULVAC-PHI, INC.) using radiation source of Al radiation with the pass energy of 224.00 eV, the radiation current of 1.0 W, and the acceleration voltage of 15 kV.

2.3. Apparatus and Procedure of CO₂ Reforming Experiment. Figure 2 shows that the experimental system setup of CO₂ reformer consists of a stainless pipe (100 mm (*H.*)×50 mm (*I.D.*)), a copper disc (50 mm (*D.*)×1 mm (*t.*)) coated with Cr- or Ag-doped TiO₂ film which is located on the teflon

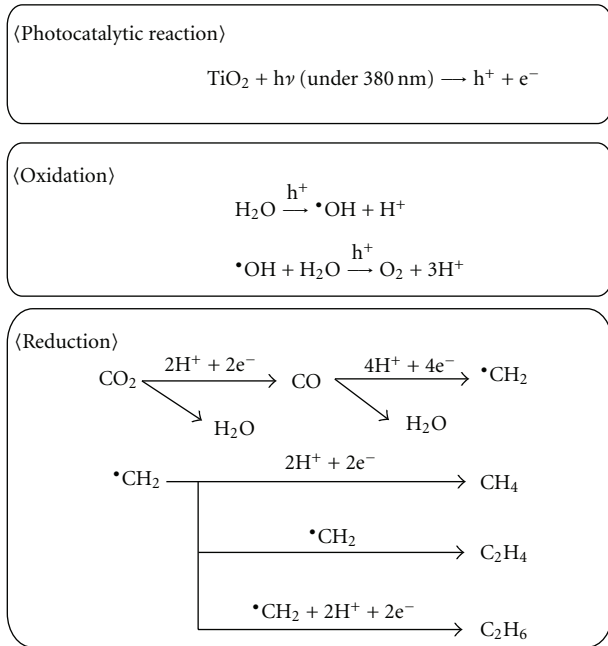


FIGURE 1: Reaction scheme of CO₂ reforming into fuel by TiO₂ photocatalyst ($\cdot\text{OH}$: hydroxy radical, $\cdot\text{CH}_2$: carbon radical).

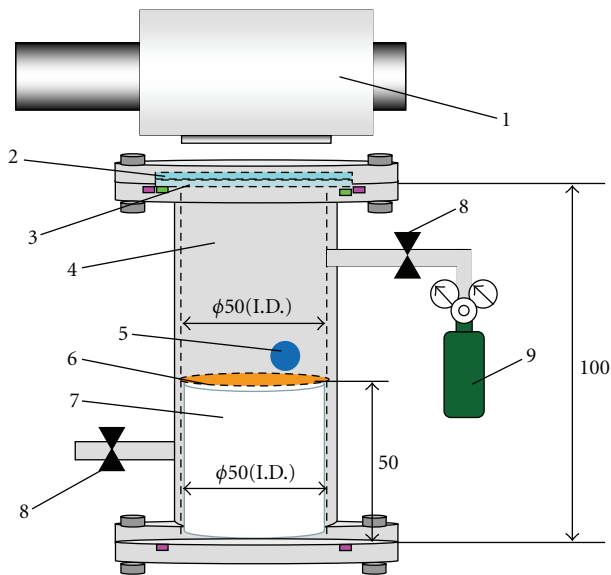


FIGURE 2: Schematic drawing of CO₂ reforming experimental system: ((1) Xe lamp; (2) coloured glass filter; (3) quartz glass disc; (4) stainless pipe; (5) gas sampling tap; (6) copper disc; (7) teflon cylinder; (8) valve; (9) CO₂ gas cylinder).

cylinder (50 mm (H.) \times 50 mm (D.)), a quartz glass disc (84 mm (D.) \times 10 mm (t.)), a coloured glass filter which cuts off the light of wavelength below 380 nm, SCF-50S-38L, SIGMA KOKI CO., LTD.), Xe lamp (L2175, Hamamatsu Photonics K. K.), and CO₂ gas cylinder. The reformer volume for CO₂ charge is $1.25 \times 10^{-4} \text{ m}^3$. Xe lamp is located over the stainless pipe. The light of Xe lamp illuminates the copper disc coated with Cr- or Ag-doped TiO₂ film, which is inserted

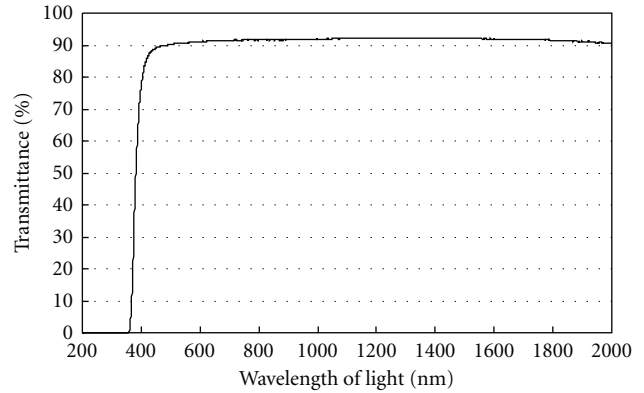


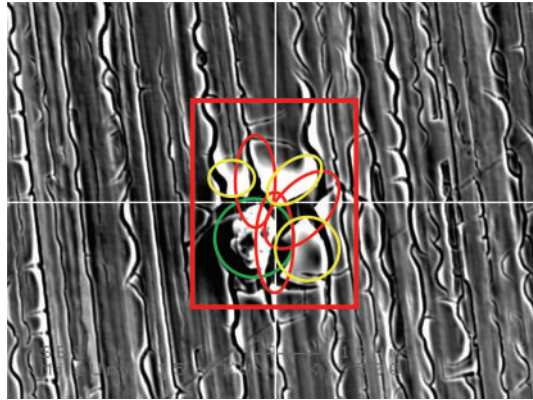
FIGURE 3: Light transmittance data of the coloured glass filter.

into the stainless pipe, through the coloured glass filter and the quartz glass disc fixed to the top of the stainless pipe. The wavelength of light from Xe lamp is ranged from 185 nm to 2000 nm. The Xe lamp can be fitted with a coloured glass filter to remove UV components of the light. With the filter, the wavelength of light from Xe lamp is ranged from 381 nm to 2000 nm. Figure 3 shows the light transmittance data of the coloured glass filter to prove the removal of the light whose wavelength is below 380 nm. The average light intensity of Xe lamp on the copper disc without and with setting the coloured glass filter is 57.53 mW/cm^2 and 43.67 mW/cm^2 , respectively.

In the CO₂ reforming experiment, CO₂ gas with the purity of 99.995 vol% was flowed through the CO₂ reformer as a purged gas for 15 minutes first. After that, the valves located at the inlet and the outlet of CO₂ reformer were closed. After confirming the gas pressure and gas temperature in the CO₂ reformer at 0.1 MPa and 298 K, respectively, the distilled water of 100 μL was injected into the CO₂ reformer, and Xe lamp illumination was turned on at the same time. The water injected vaporized completely in the reformer. Despite of the heat of UV lamp, the temperature in CO₂ reformer was kept at about 343 K during the CO₂ reforming experiment. The amount of injected water and that of CO₂ in CO₂ reformer was 5.56 mmol and 5.76 mmol, respectively. The gas in CO₂ reformer was sampled every 24 hours during the CO₂ reforming experiment. The gas samples were analyzed by FID gas chromatograph (GC353B, GL Science) and methanizer (MT221, GL Science). Minimum resolution of FID gas chromatograph and methanizer is 1 ppmV.

3. Results and Discussion

3.1. Analysis of Cr- or Ag-Doped TiO₂ Film by SEM and EPMA. Figures 4 and 5 show SEM image and EPMA image of Cr-doped TiO₂ film prepared under the condition of $R = 1 \text{ wt\%}$, respectively. Figures 6 and 7 show SEM and EPMA image of Ag-doped TiO₂ film prepared under the condition of $R = 1 \text{ wt\%}$, respectively. These SEM images were taken at 1500 times magnification under the condition of acceleration voltage of 15 kV and current of $3.0 \times 10^{-8} \text{ A}$. The red lined



— 10 μm
 $\times 1500$

FIGURE 4: SEM images of Cr-doped TiO_2 film prepared under the condition of $R = 1$ wt%.

quadrangle area in Figures 4 and 6 was used for EPMA analysis shown in Figures 5 and 7, respectively. In Figures 5 and 7, the concentration of Ti, Cu, Cr, and Ag in observation area is indicated by the difference of colour. Light colours, for example, white, pink, and red indicate that the amount of element is large, while dark colours like black, blue, and green indicate that the amount of element is small.

The green circle in Figure 4 indicates the existence of Cr particle as shown in Figure 5. Moreover, the red circles illustrated in Figure 4 indicate that the amount of Cu is also large as pointed out by the white circles in Figure 5. On the other hand, the red circle in Figure 6 indicates the existence of Ag particle as shown in Figure 7. Furthermore, the yellow circles illustrated in Figure 6 indicate that the amount of Cu is small and Ti is large as pointed out by white circles in Figure 7. These results represent the following.

- (i) Before firing process, Cr/TiO_2 or Ag/TiO_2 sol solution is adhered on the copper disc uniformly.
- (ii) During firing process, the temperature profile of Cr/TiO_2 or Ag/TiO_2 sol solution adhered on the copper disc is not even due to the difference of thermal conductivity of Ti and Cr or Ag. Their thermal conductivity of Ti, Cr, and Ag at 600 K is 19.4 W/(m·K), 80.5 W/(m·K), and 405 W/(m·K), respectively [58]. Therefore, the thermal expansion around Cr or Ag particle and the thermal shrinkage around the other areas of TiO_2 sol occur.
- (iii) Because of the thermal stress caused by the uneven distribution of temperature, the cluck around Cr or Ag and the shrinkage of TiO_2 film around the cluck occur after firing process. Therefore, a large amount of Cu, which is an element of basis copper disc, around Cr or Ag and a large amount of Ti around Cr or Ag are observed in Figures 5 and 7.

To evaluate the amount of doped Cr or Ag within TiO_2 film quantitatively, the observation area, which is the center of copper disc, of diameter of 300 μm is analysed by EPMA.

The ratio of Cr or Ag to Ti in this observation area is counted by averaging the data obtained in this area.

Table 1 indicates the relationship between each element ratio and R which is varied from 1 wt% to 100 wt% when the N is set at 1 for Cr-doped TiO_2 film. From this table, the ratio of Cr is increased with increasing R up to 70 wt% since the amount of Cr powders added into TiO_2 sol solution is increased. However, the ratio of Cr starts to decrease if the R is over 70 wt%. The reason might be that when the amount of Cr powders in TiO_2 sol solution was too much, the shrinkage of TiO_2 film occurred. Therefore, the fixing strength of TiO_2 film to copper disc was weakened, resulting in the ratio of Cr being decreased for R over 70 wt%. The ratio of Cr to Ti shown in Table 1, which is measured value, is different from the calculated R from the Cr powders added into TiO_2 sol solution because of the agglomeration of Cr powders in TiO_2 sol solution. Although Cr powders in TiO_2 sol solution were mixed by magnetic stirrer well and the powders were stored under no moisture condition before the experiment, it was still difficult to prevent it from the agglomeration for such a fine particle completely.

Table 2 indicates the relationship between each element ratio and R which is varied from 1 wt% to 50 wt% when the N is set at 1 for Ag-doped TiO_2 film. From this table, the ratio of Ag is increased with increasing R up to 50 wt% since the amount of Ag powders added into TiO_2 sol solution is increased. However, the increase ratio of Ag is not so large compared to the exact amount of Ag powders added into TiO_2 sol solution. The density of Ag which is 10787 kg/m³ is much larger than the density of Ti which is 4507 kg/m³. Although TiO_2 sol solution was mixed by magnetic stirrer well during dip-coating process, most of Ag particles were liable to sink in TiO_2 sol solution in dip-coating process. Especially, for the case that R is over 10 wt%, the amount of Ag detected by EPMA is so small compared to the amount of Ag powders added into TiO_2 sol solution, resulting in the fact that the control of doping a large amount of Ag by sol-gel and dip-coating process is quite difficult. The SEM image, that is, Figure 8, of Ag-doped TiO_2 film prepared under the condition of $R = 50$ wt% shows that there are many holes and clucks on TiO_2 film, which are indicated by pink circles. However, fewer holes and clucks are seen in SEM image of Ag-doped TiO_2 film prepared under the condition of $R = 1$ wt% as shown in Figure 6. It is thought that these holes and clucks in Figure 8 are caused by peeling off TiO_2 film. In addition, from EPMA image of Ag-doped TiO_2 film prepared under the condition of $R = 50$ wt% shown in Figure 9, it can be seen that there are some areas where the amount of Cu is large while the amount of Ti is small. These areas is pointed out by white circles, while Ag in surrounding areas are pointed out by red circles. This result is thought to be caused by peeling off TiO_2 film around Ag particles. However, no such areas where the amount of Cu is large while the amount of Ti is small are observed in EPMA image of Ag-doped TiO_2 film prepared under the condition of $R = 1$ wt% as shown in Figure 7. Therefore, it can be concluded that the peeling off TiO_2 film with Ag particles in dip-coating process only occurs under high R condition.

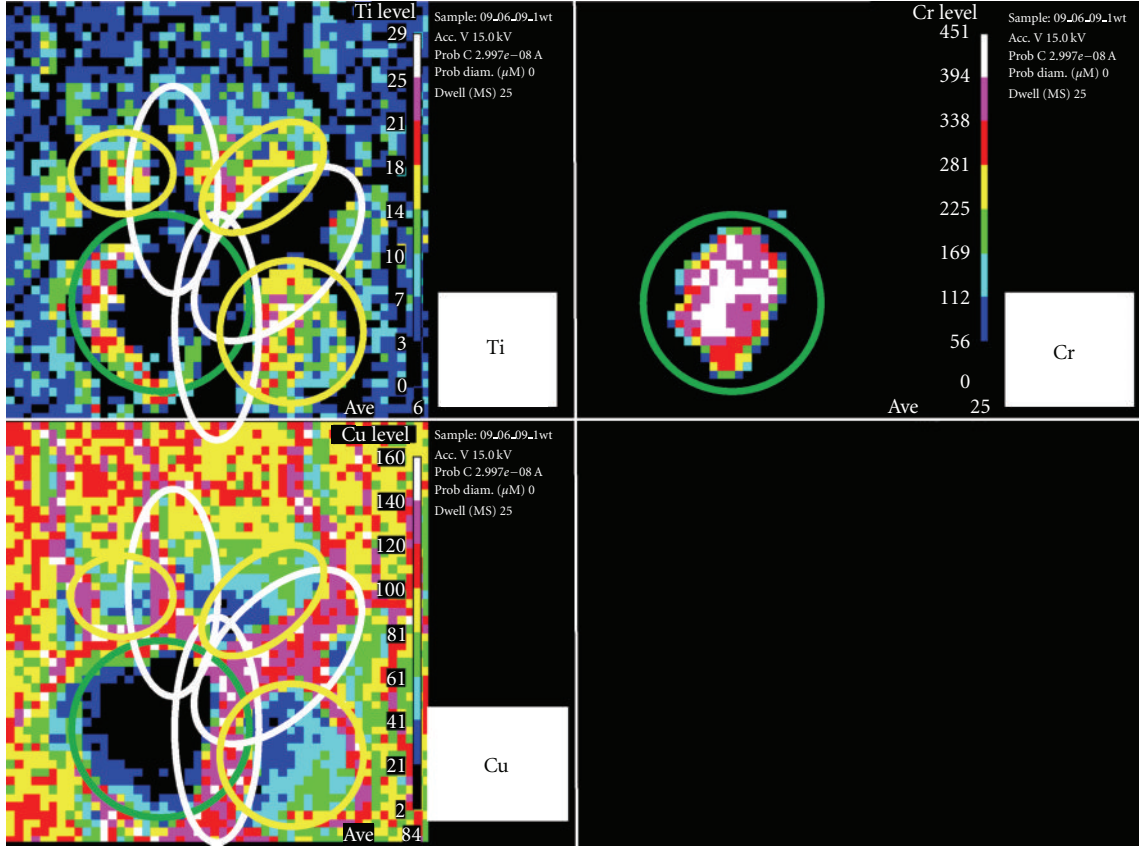


FIGURE 5: EPMA image of Cr-doped TiO_2 film prepared under the condition of $R = 1$ wt%.

TABLE 1: Relationship between each element and different R for Cr-doped TiO_2 film.

R [wt%]	1	10	20	30	40	50	60	70	80	90	100
Element											
Cr [wt%]	5.5	7.1	8.2	11.3	13.2	15.3	18.9	22.4	17.0	18.0	18.6
Ti [wt%]	94.5	92.9	91.8	88.7	86.8	84.7	81.1	77.6	83.0	82.0	81.4
Total	100.0	100.0	100.0	100.0	100.0	100.0	100.0	100.0	100.0	100.0	100.0

TABLE 2: Relationship between each element and different R for Ag-doped TiO_2 film.

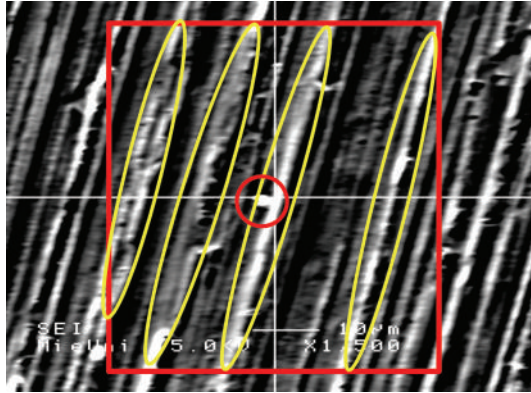
R [wt%]	1	10	20	30	40	50
Element						
Ag [wt%]	0.6	1.4	1.9	2.5	2.6	3.4
Ti [wt%]	99.4	98.6	98.1	97.5	97.4	96.6
Total	100.0	100.0	100.0	100.0	100.0	100.0

3.2. Investigation of the Optimum Doping Ratio of Cr and Ag.

Figure 10 shows the concentration changes of CO produced by CO_2 reforming along the time under the Xe lamp with UV light on, for several Cr- or Ag-doped TiO_2 films prepared under the different R conditions. In this experiment, CO is the only fuel produced from CO_2 reforming. Since the concentration of CO started to decrease after illumination of 72 hours for every R , Figure 10 only shows the concentration

up to 72 hours. Before this CO_2 reforming experiment, a blank test, that is, running the CO_2 reforming experiment without illumination of Xe lamp, has been carried out to set up a reference case. No fuel was produced in the blank test as expected.

According to Figure 10, the concentration of CO is increased with increasing R up to 70 wt% for Cr-doped TiO_2 film. As Table 1 indicates that the ratio of Cr is also increased with increasing R up to 70 wt%, the result of CO_2 reforming experiment matches well with the result of EPMA analysis. On the other hand, it is revealed that the concentration of CO for $R = 1$ wt% which is larger than that for $R = 50$ wt% though the amount of Ag detected by EPMA for $R = 50$ wt% is larger than that for $R = 1$ wt% as shown in Table 2. The reason to cause this result might be that TiO_2 film was peeled off with Ag particles in dip-coating process especially under high R condition. Since the density of Ag is larger than that of Ti, TiO_2 sol solution cannot keep Ag particles on copper disc



— 10 μm
 ×1500

FIGURE 6: SEM image of Ag-doped TiO_2 film prepared under the condition of $R = 1$ wt%.

by its viscosity during dip-coating process. When Ag particles drop, TiO_2 sol solution or TiO_2 film around Ag particles drops together. Therefore, the CO_2 reforming performance of $R = 50$ wt% is lower than that of $R = 1$ wt%.

To verify the photoresponse extension of TiO_2 to the visible spectrum by Cr or Ag doping, Figure 11 shows the concentration change of CO with illumination time of Xe lamp without UV light for several Cr- or Ag-doped TiO_2 film prepared under different R conditions. In this figure, the data for $R = 0$ wt%, 50 wt%, 70 wt%, and 100 wt% are shown for Cr-doped TiO_2 film. This figure includes the concentration change with illumination time of Xe lamp without UV light more than 72 hours, since it was thought that the time to attain the peak concentration might be longer than that under Xe lamp with UV light [51, 59].

It is seen that the concentration of CO for $R = 0$ wt% keeps 0 ppmV. Therefore, it means that the prepared TiO_2 film without doping does not have the photoresponse ability of visible spectrum. On the other hand, Cr- or Ag-doped TiO_2 film shows the photoresponse ability of visible spectrum since the CO is detected. As to the results of Cr-doped TiO_2 film, it reveals that $R = 70$ wt% is the best that agrees with the results shown in Table 1 and Figure 10. However, the peak concentration level of CO without UV light is lower than that with UV light. The results on Ag-doped TiO_2 film reveal that $R = 50$ wt% is better than $R = 1$ wt% in the experiment without UV light illumination though the difference between $R = 50$ wt% and $R = 1$ wt% is small.

The following points can be thought to explain these results.

- (i) The CO_2 reforming performance is improved by Cr or Ag doping since the photoresponse ability of visible spectrum is realized. The light energy which can be used for CO_2 reforming is increased.
- (ii) On the other hand, the CO_2 reforming performance can also be declined by Cr or Ag doping since the

recombination of hole and electron occurs. Though it is thought that sol-gel and dip-coating process can incorporate dopants into the TiO_2 lattice without lattice defect [47], the lattice defect which causes the recombination of hole and electron might have occurred in this study.

- (iii) The CO_2 reforming performance would be improved by Cr or Ag doping if the recombination of hole and electron could be prevented. According to the previous reports [1, 5, 7, 11–17], a metal loading is usually adopted to prevent the recombination of electron and hole under the condition of illumination of UV light.

Considering the CO_2 reforming performance of Cr-doped TiO_2 film, the data shown in Table 1, Figures 10 and 11 are analyzed based on the above three points as follows.

- (I) From Figure 10 that the concentrations of CO for $R = 1$ wt% and 10 wt% are lower than that for $R = 0$ wt%. It is thought that the above described (ii) should have occurred in this experiment. Therefore, there is a minimum amount of Cr doping existing in order to improve the CO_2 reforming performance of TiO_2 .
- (II) As shown in Figure 10, the concentration of CO for R over 30 wt% is bigger than that for $R = 0$ wt%. If the above described points (i) to (iii) were all in effect equally, the concentration of CO should not increase. Therefore, it is thought that the point (i) or (iii) should be dominant until R is up to 70 wt% as shown in Table 1.
- (III) It can be seen from Figure 10 that the concentration of CO for R over 90 wt% is low. The reason is thought to be that when R is too high, Cr powders with TiO_2 might be removed away from copper disc surface that is not in contact with the disc during dip-coating process. Although the amount of Cr powders in TiO_2 sol solution is increased under high R conditions, the Cr in contact with copper disc might be decreased because the amount of Cr powders being removed from copper disc might increase more. Therefore, as a result, the CO_2 reforming performance for R over 90 wt% is declined.
- (IV) Comparing Figure 10 with Figure 11, the concentration of CO under visible light (i.e. without UV light) is lower than that under the UV light. It is thought that Cr doping has two effects on the CO_2 reforming performance: (1) prevention of recombination of electron and hole under UV light and (2) extension of photoresponse ability into visible spectrum. The results in Figures 10 and 11 show that the effect of preventing the recombination of electron and hole under UV light is stronger than that of extending photoresponse ability to the visible spectrum.

For the effect on the CO_2 reforming performance by the Ag-doped TiO_2 film, the results are shown in Table 2, Figures 10 and 11. From the results, it can be seen that

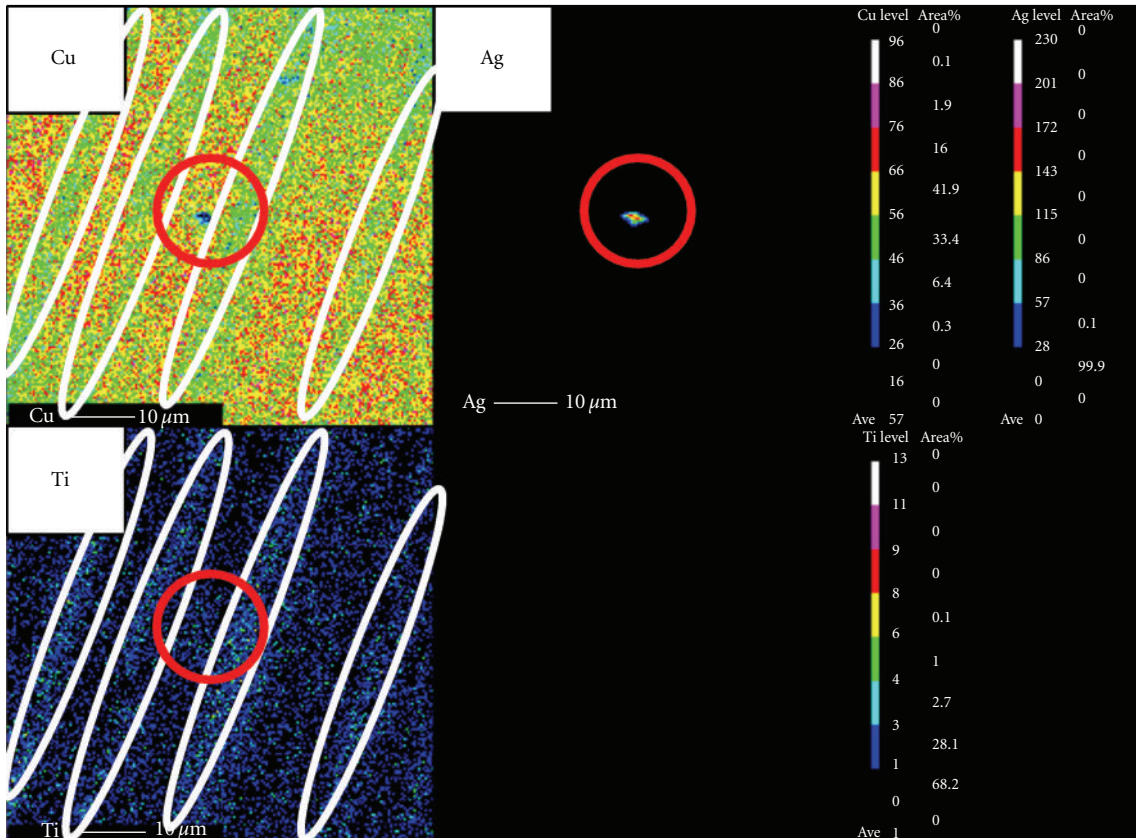
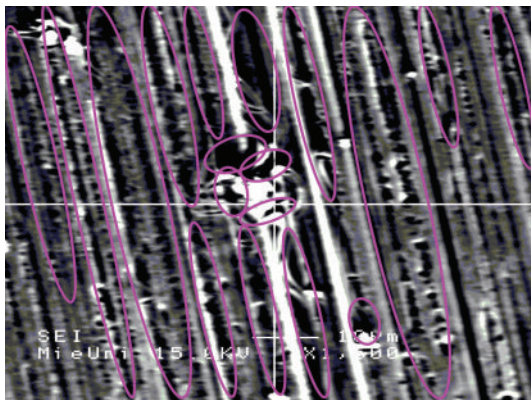


FIGURE 7: EPMA image of Ag-doped TiO₂ film prepared under the condition of $R = 1$ wt%.



— 10 μm
×1500

FIGURE 8: SEM image of Ag-doped TiO₂ film prepared under the condition of $R = 50$ wt%.

the CO₂ reforming performance of $R = 50$ wt% is better than that of $R = 1$ wt% if without UV light illumination, while the CO₂ reforming performance of $R = 1$ wt% is better than that of $R = 50$ wt% if with UV light illumination. The CO₂ reforming performance without UV light is generally lower than that with UV light irrespective of R . For example, when $R = 50$ wt% after illumination of Xe lamp of 72 hours, the

CO₂ reforming performance without UV light is about thirty seventh part of that with UV light. The amount of Ag and the ratio of amount of TiO₂ film to doped Ag are important to improve the photoresponse ability of doped TiO₂ film, as shown in Figure 10. Therefore, $R = 1$ wt% is selected as the optimum condition for Ag doping in this study as it gives the best result as shown in Figure 10. Another point to be noted is that, compared with Cr doping, Ag doping is much more effective to promote the CO₂ reforming performance under the conditions with or without UV light.

3.3. Effect of Coating Number of Cr- or Ag-Doped TiO₂ Film on CO₂ Reforming Characteristics. Since the product of the CO₂ reforming is only CO in this experiment, it is thought that the reduction effect of TiO₂ is not so strong according to the reaction scheme shown in Figure 1. From Figure 1, more electron and proton are necessary to produce hydrocarbons like CH₄, C₂H₄, and C₂H₆. When the reduction effect of TiO₂ is promoted, the concentration of CO which is a pre-product to the hydrocarbons is also increased. The previous studies [48–51] show that the increase in N is effective to promote the reduction performance of TiO₂ photocatalyst due to increase of the amount of TiO₂. Under the higher N condition, more electrons are produced by photocatalytic reaction. The effect of N of Cr- or Ag-doped TiO₂ film on CO₂ reforming performance and photoresponse ability of visible spectrum is investigated further below.

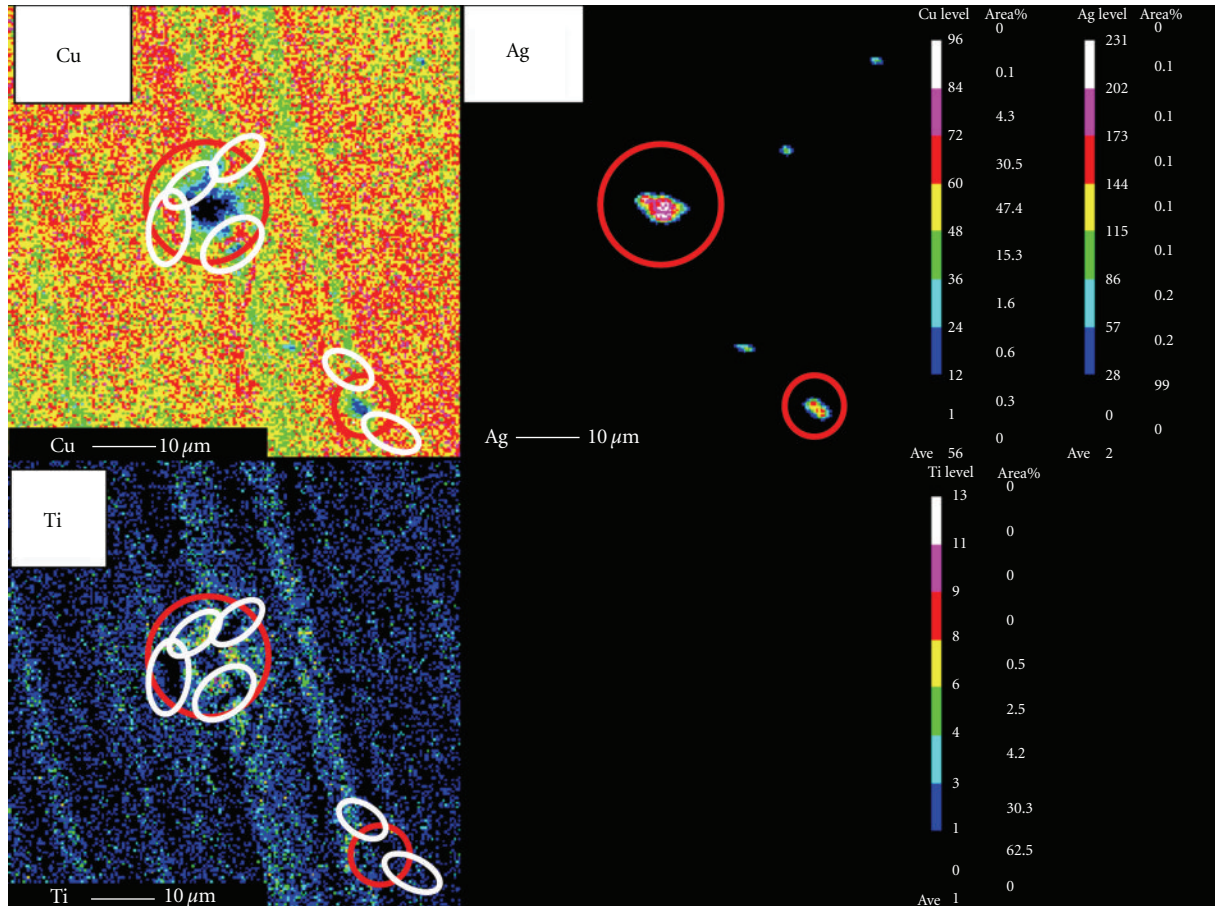


FIGURE 9: EPMA image of Ag-doped TiO₂ film prepared under the condition of $R = 50$ wt%.

Figure 12 shows the concentrations of products from the CO₂ reforming after illumination of Xe lamp with UV light of 72 hours for several Cr-doped TiO₂ film prepared under conditions of different N . In this experiment, two coating conditions were investigated: Cr is doped in every layer (N_{all}) and Cr is doped only in the top layer (N_{top}), while R is fixed at 70 wt% in doping. Figure 12 indicates that the total concentration of products is increased with increasing N , since the amount of Cr-doped TiO₂ film coated on copper disc becomes larger with increasing N . However, the degree of the increase in N for N_{top} cases is higher than that for N_{all} cases. In addition, it is seen that CH₄ and C₂H₆ as well as CO are produced more for N_{top} cases compared with N_{all} cases. This might be caused by the clucks occurring after finishing firing process. Each layer that is the base for next upper layer coating is weaker in N_{all} cases, resulting in the fact that the uniform coating for each layer is difficult to achieve. However, it is thought that the coating layers before the last coating are kept uniform in N_{top} cases. The reason why the concentrations of CH₄ and C₂H₆ are increased with increasing N in N_{top} cases is thought to be the increase in the amount of TiO₂.

Figure 13 shows the concentrations of products from CO₂ reforming after illumination of Xe lamp with UV light of 72 hours for several Ag-doped TiO₂ films prepared under

TABLE 3: Relationship between each element and different N for Ag-doped TiO₂ film.

N	$N_{\text{all}} = 1$	$N_{\text{all}} = 3$	$N_{\text{top}} = 3$	$N_{\text{top}} = 5$
Element				
Ag [wt%]	0.6	2.4	0.6	0.6
Ti [wt%]	99.4	97.6	99.4	99.4
Total	100.0	100.0	100.0	100.0

conditions of different N . In this experiment, R is fixed at 1 wt% in doping. And the results of N_{all} and N_{top} are shown in this figure. The data of other hydrocarbons, which were detected for every R , are omitted in this figure since the values of them are below 50 ppmV. From Figure 13, the best result is when $N_{\text{all}} = 1$, though EPMA analysis shown in Table 3 reveals that the largest amount of Ag detected is obtained when $N_{\text{all}} = 3$ under the experimental conditions. When N is same, the ratio of detected Ag to total element for N_{all} is larger than that for N_{top} . Although a good promotion of CO₂ reforming performance was expected by EPMA analysis, $N_{\text{all}} = 3$ does not show the good CO₂ reforming performance. In addition, the result of N_{top} is superior to the result of N_{all} . Under the condition of N_{all} , TiO₂ film is liable to be removed by increasing N since

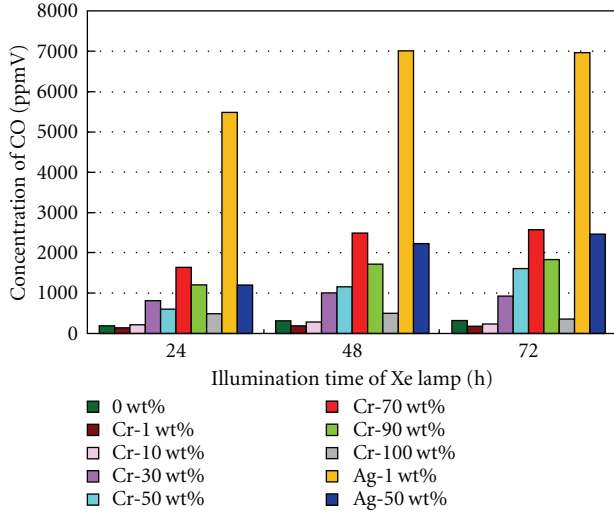


FIGURE 10: Comparison of produced concentration of CO among different R under the condition of illuminating Xe lamp with UV light.

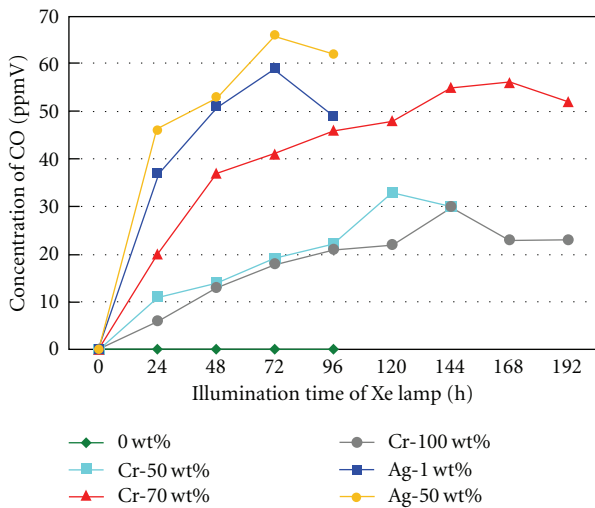


FIGURE 11: Comparison of produced concentration of CO among different R under the condition of illuminating Xe lamp without UV light.

doped Ag particles cause the uneven thin TiO₂ film on the former coated TiO₂ film and make TiO₂ film weak. Since Ag-doped TiO₂ film detaches, the amount of coated TiO₂ is decreased. On the other hand, under the condition of N_{top} , it is thought that even and steady thin TiO₂ film is coated more easily than N_{all} . Therefore, the CO₂ reforming performance of $N_{top} = 3$ is better than that of $N_{all} = 3$. However, the CO₂ reforming performance of $N_{top} = 5$ is worse compared with that of $N_{top} = 3$. It might be a result that doped Ag particles cause clucks of TiO₂ film during dip-coating process due to thermal stress. In the last coating, the former coated TiO₂ film under many N condition is weaker than that under small N condition, since the copper disc that is harder than TiO₂ film separates from the former

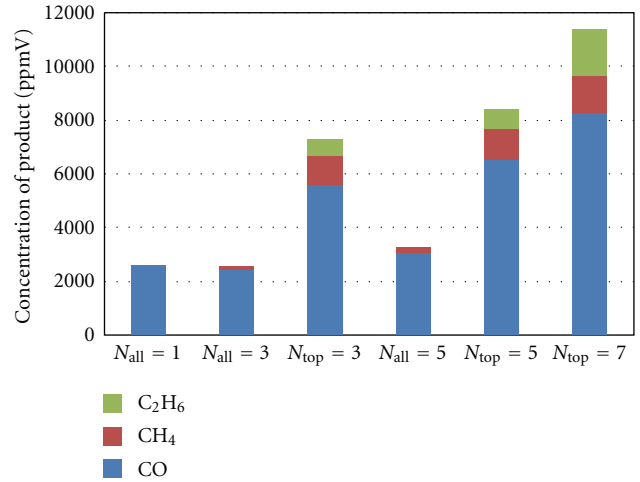


FIGURE 12: Comparison of product by CO₂ reforming after illumination of Xe lamp with UV light of 72 h for several Cr-doped TiO₂ film prepared under conditions of different N .

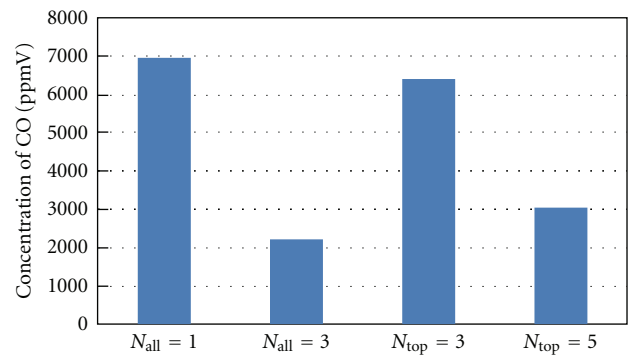


FIGURE 13: Comparison of product by CO₂ reforming after illumination of Xe lamp with UV light of 72 h for several Ag-doped TiO₂ film prepared under conditions of different N .

coated TiO₂ film by coating repetition. Therefore, the CO₂ reforming performance is worse with increasing N to 5. According to Figure 14 which shows the results without UV light, the CO₂ reforming performances of $N_{top} = 3$ and $N_{all} = 3$ are inferior to that of $N_{all} = 1$. Consequently, as to Ag doping, the N number seems having no impact on CO₂ reforming performance under both with and without UV conditions. Since the difference of thermal conductivities between Ag and Ti is larger than that between Cr and Ti, it is thought that the thermal stress becomes larger for Ag doping when N increases. By comparing all the results, the best CO₂ reforming was achieved under the condition of the $N_{top} = 7$ with Cr doping in this study. Consequently, the large effect of many N on CO₂ reforming performance is obtained for Cr doping.

After illumination of Xe lamp with UV light of 72 hours, the concentration of CO, CH₄, and C₂H₆ can reach 8306 ppmV (= 92.5 mmol/g-catalyst), 1367 ppmV

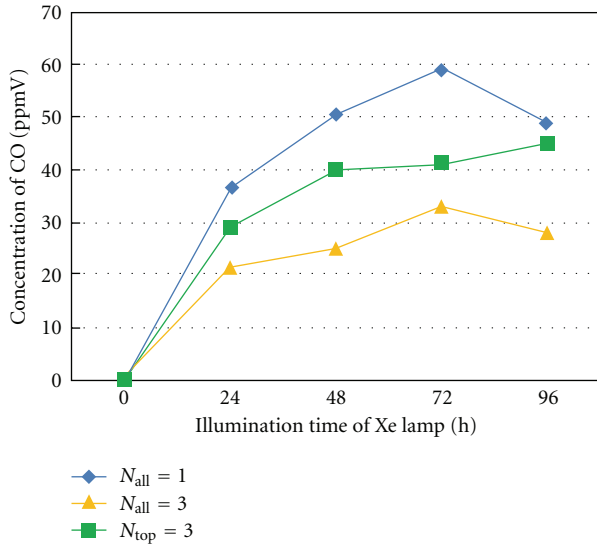


FIGURE 14: Comparison of concentration change of CO by CO₂ reforming with illumination time of Xe lamp without UV light for $N_{all} = 1$, $N_{all} = 3$ and $N_{top} = 3$.

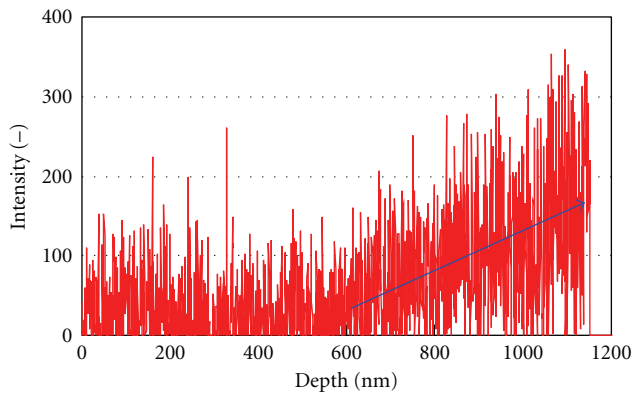


FIGURE 15: Cu element profile through thickness direction of the Cr-doped TiO₂ film under the condition of $N_{top} = 7$ by XPS analysis.

(= 15.2 mmol/g-catalyst), and 1712 ppmV (= 19.1 mmol/g-catalyst), respectively, where the method to calculate the amount of product per weight of catalyst is as follows.

The thickness of Cr-doped TiO₂ film should be measured first, and then with the known surface area of copper disc of $1.96 \times 10^{-3} \text{ m}^2$ and the density of TiO₂ of 3900 kg/m^3 [60], the mass of TiO₂ can be calculated. XPS analysis was used to measure the thickness of Cr-doped TiO₂ film. Figure 15 shows the Cu element profile through thickness direction of the Cr-doped TiO₂ film in the case of $N_{top} = 7$ by the XPS analysis. XPS spectra of Cu 3p are detected. In this XPS analysis, the sputtering rate is about 0.8 nm/min. It is seen that the intensity of Cu is increased dramatically from about 600 nm in this case. It alludes to the fact that the basis copper disc is at the depth of 600 nm; that is, the thickness of the TiO₂ film is 600 nm. In this calculation, the weight of Cr has been ignored since Cr was doped in the top layer only.

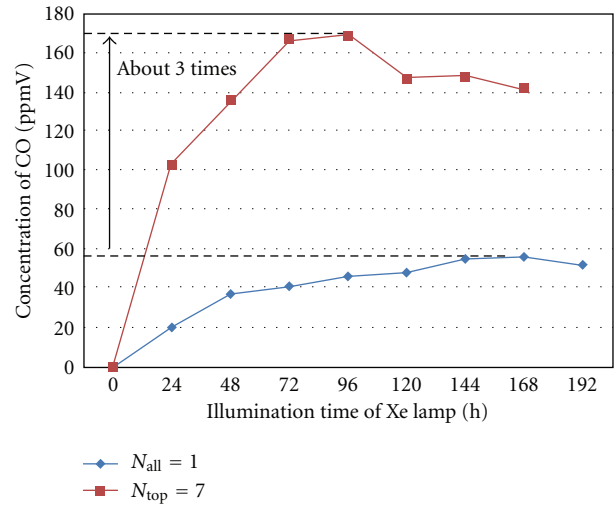


FIGURE 16: Comparison of concentration change of CO by CO₂ reforming with illumination time of Xe lamp without UV light for $N_{all} = 7$ and $N_{top} = 7$.

To verify the effect of photoresponse extension of TiO₂ to the visible spectrum for $N_{top} = 7$ in Cr coating, Figure 16 shows the results obtained with illumination time of Xe lamp without UV light. The data for $N_{all} = 1$ under $R = 70 \text{ wt}\%$ is also shown in this figure for comparison. Although CH₄ is produced from the experiment for $N_{top} = 7$, the concentration is below 10 ppmV. Therefore, Figure 16 shows the concentration of CO only. The peak value of concentration of CO for $N_{top} = 7$ is about 3 times as large as that of $N_{all} = 1$. This proves that in the case of $N_{top} = 7$, the photoresponse ability of visible spectrum is also promoted by the increase of the amount of TiO₂ and the converted Cr ion-like Cr³⁺ brought by encouragement of reduction performance of photocatalyst. Given that the concentration of product for $R = 0 \text{ wt}\%$ is at such a low level as shown in Figures 10 and 11, it can be concluded that CO₂ reforming performance of TiO₂ is promoted dramatically by Cr doping. In the research by Ozcan et al. [24] which tried to extend the photoresponse of TiO₂ to the visible spectrum by Pt loading, the amount of product from CO₂ reforming without UV light was 104 times less than what we produced in this study. Therefore, Cr doping by sol-gel and dip-coating process is effective to promote the CO₂ reforming performance of TiO₂.

4. Conclusions

Based on the experimental results, the following conclusions can be drawn from this study.

Both Cr doping and Ag doping can promote the CO₂ reforming performance by TiO₂. The optimum R when $N = 1$ for Cr doping and Ag doping is 70 wt% and 1 wt%, respectively. Since the density of Ag is much larger than the density of Ti, the amount of Ag doped on TiO₂ film is lower compared to the actual amount of Ag powders added into TiO₂ sol solution, resulting in the fact that the good

CO₂ reforming performance is not obtained under large *R* condition. The promotion of CO₂ reforming performance by Cr or Ag doping comes from two aspects: (1) the photoresponse ability being extended to visible spectrum by the doping, and (2) doping preventing the recombination of electron and hole if there is UV light. The latter is stronger than the former. The best result obtained is in the case of $N_{\text{top}} = 7$ with Cr doping under the investigated conditions in this study.

Acknowledgment

The authors gratefully acknowledge the financial support from Tanikawa Fund Promotion of Thermal Technology.

References

- [1] K. Adachi, K. Ohta, and T. Mizuno, "Photocatalytic reduction of carbon dioxide to hydrocarbon using copper-loaded titanium dioxide," *Solar Energy*, vol. 53, no. 2, pp. 187–190, 1994.
- [2] M. Anpo and K. Chiba, "Photocatalytic reduction of CO₂ on anchored titanium oxide catalysts," *Journal of Molecular Catalysis*, vol. 74, pp. 207–212, 1992.
- [3] B. Aurian-Blajeni, M. Halmann, and J. Manassen, "Photoreduction of carbon dioxide and water into formaldehyde and methanol on semiconductor materials," *Solar Energy*, vol. 25, no. 2, pp. 165–170, 1980.
- [4] G. R. Dey, A. D. Belapurkar, and K. Kishore, "Photo-catalytic reduction of carbon dioxide to methane using TiO₂ as suspension in water," *Journal of Photochemistry and Photobiology A*, vol. 163, no. 3, pp. 503–508, 2004.
- [5] K. Hirano, K. Inoue, and T. Yatsu, "Photocatalysed reduction of CO₂ in aqueous TiO₂ suspension mixed with copper powder," *Journal of Photochemistry and Photobiology A*, vol. 64, no. 2, pp. 255–258, 1992.
- [6] T. Inoue, A. Fujishima, S. Konishi, and K. Honda, "Photoelectrocatalytic reduction of carbon dioxide in aqueous suspensions of semiconductor powders," *Nature*, vol. 277, no. 5698, pp. 637–638, 1979.
- [7] O. Ishitani, C. Inoue, Y. Suzuki, and T. Ibusuki, "Photocatalytic reduction of carbon dioxide to methane and acetic acid by an aqueous suspension of metal-deposited TiO₂," *Journal of Photochemistry and Photobiology A*, vol. 72, pp. 269–271, 1993.
- [8] S. Kaneco, H. Kurimoto, Y. Shimizu, K. Ohta, and T. Mizuno, "Photocatalytic reduction of CO₂ using TiO₂ powders in supercritical fluid CO₂," *Energy*, vol. 24, no. 1, pp. 21–30, 1999.
- [9] K. Ogura, M. Kawano, J. Yano, and Y. Sakata, "Visible-light-assisted decomposition of H₂O and photomethanation of CO₂ over CeO₂-TiO₂ catalyst," *Journal of Photochemistry and Photobiology A*, vol. 66, no. 1, pp. 91–97, 1992.
- [10] K. Takeuchi, S. Murasawa, and T. Ibusuki, *World of Photocatalyst*, Kougyouchousakai, Tokyo, Japan, 2001.
- [11] Z. Goren, I. Willner, A. J. Nelson, and A. J. Frank, "Selective photoreduction of CO₂/HCO₃⁻ to formate by aqueous suspensions and colloids of Pd-TiO₂," *Journal of Physical Chemistry*, vol. 94, no. 9, pp. 3784–3790, 1990.
- [12] M. Halmann, V. Katzir, E. Borgarello, and J. Kiwi, "Photoassisted carbon dioxide reduction on aqueous suspensions of titanium dioxide," *Solar Energy Materials*, vol. 10, no. 1, pp. 85–91, 1984.
- [13] T. Ibusuki, "Reduction of CO₂ by photocatalyst," *Syokubai*, vol. 35, pp. 506–512, 1993.
- [14] K. Kawano, T. Uehara, H. Kato, and K. Hirano, "Photocatalysed reduction of CO₂ in aqueous TiO₂ suspension mixed with various metal powder," *Kagaku to Kyoiku*, vol. 41, pp. 766–770, 1993.
- [15] C. C. Lo, C. H. Hung, C. S. Yuan, and J. F. Wu, "Photoreduction of carbon dioxide with H₂ and H₂O over TiO₂ and ZrO₂ in a circulated photocatalytic reactor," *Solar Energy Materials and Solar Cells*, vol. 91, no. 19, pp. 1765–1774, 2007.
- [16] I. H. Tseng, W. C. Chang, and J. C. S. Wu, "Photoreduction of CO₂ using sol-gel derived titania and titania-supported copper catalysts," *Applied Catalysis B*, vol. 37, no. 1, pp. 37–48, 2002.
- [17] H. Yamashita, H. Nishiguchi, N. Kamada, and M. Anpo, "Photocatalytic reduction of CO₂ with H₂O on TiO₂ and Cu/TiO₂ catalysts," *Research on Chemical Intermediates*, vol. 20, pp. 815–823, 1994.
- [18] P. Pathak, M. J. Mezziani, Y. Li, L. T. Cureton, and Y. P. Sun, "Improving photoreduction of CO₂ with homogeneously dispersed nanoscale TiO₂ catalysts," *Chemical Communications*, vol. 10, no. 10, pp. 1234–1235, 2004.
- [19] J. Qu, X. Zhang, Y. Wang, and C. Xie, "Electrochemical reduction of CO₂ on RuO₂/TiO₂ nanotubes composite modified Pt electrode," *Electrochimica Acta*, vol. 50, no. 16–17, pp. 3576–3580, 2005.
- [20] X. H. Xia, Z. J. Jia, Y. Yu, Y. Liang, Z. Wang, and L. L. Ma, "Preparation of multi-walled carbon nanotube supported TiO₂ and its photocatalytic activity in the reduction of CO₂ with H₂O," *Carbon*, vol. 45, no. 4, pp. 717–721, 2007.
- [21] F. Cecchet, M. Alebbi, C. A. Bignozzi, and F. Paolucci, "Efficiency enhancement of the electrocatalytic reduction of CO₂: fac-[Re(v-bpy)(CO)₃Cl] electropolymerized onto mesoporous TiO₂ electrodes," *Inorganica Chimica Acta*, vol. 359, no. 12, pp. 3871–3874, 2006.
- [22] L. F. Cueto, G. A. Hirata, and E. M. Sánchez, "Thin-film TiO₂ electrode surface characterization upon CO₂ reduction processes," *Journal of Sol-Gel Science and Technology*, vol. 37, no. 2, pp. 105–109, 2006.
- [23] J. C. S. Wu and H. M. Lin, "Photo reduction of CO₂ to methanol via TiO₂ photocatalyst," *International Journal of Photoenergy*, vol. 7, no. 3, pp. 115–119, 2005.
- [24] O. Ozcan, F. Yukruk, E. U. Akkaya, and D. Uner, "Dye sensitized CO₂ reduction over pure and platinumized TiO₂," *Topics in Catalysis*, vol. 44, no. 4, pp. 523–528, 2007.
- [25] M. Kitano, M. Matsuoka, M. Ueshima, and M. Anpo, "Recent developments in titanium oxide-based photocatalysts," *Applied Catalysis A*, vol. 325, no. 1, pp. 1–14, 2007.
- [26] M. Kitano, M. Takeuchi, M. Matsuoka, J. M. Thomas, and M. Anpo, "Photocatalytic water splitting using Pt-loaded visible light-responsive TiO₂ thin film photocatalysts," *Catalysis Today*, vol. 120, no. 2, pp. 133–138, 2007.
- [27] X. Yang, C. Cao, K. Hohn et al., "Highly visible-light active C- and V-doped TiO₂ for degradation of acetaldehyde," *Journal of Catalysis*, vol. 252, no. 2, pp. 296–302, 2007.
- [28] R. Dholam, N. Patel, M. Adami, and A. Miotello, "Hydrogen production by photocatalytic water-splitting using Cr- or Fe-doped TiO₂ composite thin films photocatalyst," *International Journal of Hydrogen Energy*, vol. 34, no. 13, pp. 5337–5346, 2009.
- [29] T. Kamegawa, J. Sonoda, K. Sugimura, K. Mori, and H. Yamashita, "Degradation of isobutanol diluted in water over visible light sensitive vanadium doped TiO₂ photocatalyst," *Journal of Alloys and Compounds*, vol. 486, no. 1–2, pp. 685–688, 2009.
- [30] Y. Xie, Q. Zhao, X. J. Zhao, and Y. Li, "Low temperature preparation and characterization of N-doped and N-S-codoped

- TiO₂ by sol-gel route,” *Catalysis Letters*, vol. 118, no. 3-4, pp. 231–237, 2007.
- [31] D. Li, N. Ohashi, S. Hishita, T. Kolodiazny, and H. Haneda, “Origin of visible-light-driven photocatalysis: a comparative study on N/F-doped and N-F-codoped TiO₂ powders by means of experimental characterizations and theoretical calculations,” *Journal of Solid State Chemistry*, vol. 178, no. 11, pp. 3293–3302, 2005.
- [32] A. Fujishima, X. Zhang, and D. A. Tryk, “TiO₂ photocatalysis and related surface phenomena,” *Surface Science Reports*, vol. 63, no. 12, pp. 515–582, 2008.
- [33] W. Choi, A. Termin, and M. R. Hoffmann, “The role of metal ion dopants in quantum-sized TiO₂: correlation between photoreactivity and charge carrier recombination dynamics,” *Journal of Physical Chemistry*, vol. 98, no. 51, pp. 13669–13679, 1994.
- [34] J. Zhu, Z. Deng, F. Chen et al., “Hydrothermal doping method for preparation of Cr³⁺-TiO₂ photocatalysts with concentration gradient distribution of Cr³⁺,” *Applied Catalysis B*, vol. 62, no. 3-4, pp. 329–335, 2006.
- [35] J. A. Navio, G. Colon, M. I. Litter, and G. N. Bianco, “Synthesis, characterization and photocatalytic properties of ion-doped titanium semiconductors prepared from TiO₂ and iron (III) acetylacetonate,” *Journal of Molecular Catalysis A*, vol. 106, no. 3, pp. 267–276, 1996.
- [36] J. Zhu, W. Zheng, B. He, J. Zhang, and M. Anpo, “Characterization of Fe-TiO₂ photocatalysts synthesized by hydrothermal method and their photocatalytic reactivity for photodegradation of XRG dye diluted in water,” *Journal of Molecular Catalysis A*, vol. 216, no. 1, pp. 35–43, 2004.
- [37] M. Anpo, “Preparation, characterization, and reactivities of highly functional titanium oxide-based photocatalysts able to operate under UV-visible light irradiation: approaches in realizing high efficiency in the use of visible light,” *Bulletin of the Chemical Society of Japan*, vol. 77, no. 8, pp. 1427–1442, 2004.
- [38] M. Anpo and M. Takeuchi, “The design and development of highly reactive titanium oxide photocatalysts operating under visible light irradiation,” *Journal of Catalysis*, vol. 216, no. 1-2, pp. 505–516, 2003.
- [39] J.-M. Herrmann, J. Disdier, and P. Pichat, “Effect of chromium doping on the electrical and catalytic properties of powder titania under UV and visible illumination,” *Chemical Physics Letters*, vol. 108, no. 6, pp. 618–622, 1984.
- [40] H. Kato and A. Kudo, “Visible-light-response and photocatalytic activities of TiO₂ and SrTiO₃ photocatalysts codoped with antimony and chromium,” *Journal of Physical Chemistry B*, vol. 106, no. 19, pp. 5029–5034, 2002.
- [41] M. Anpo, M. Takeuchi, K. Ikeue, and S. Dohshi, “Design and development of titanium oxide photocatalysts operating under visible and UV light irradiation. The applications of metal ion-implantation techniques to semiconducting TiO₂ and Ti/zeolite catalysts,” *Current Opinion in Solid State and Materials Science*, vol. 6, no. 5, pp. 381–388, 2002.
- [42] T. Sumita, T. Yamaki, S. Yamamoto, and A. Miyashita, “Photo-induced surface charge separation in Cr-implanted TiO₂ thin film,” *Thin Solid Films*, vol. 416, no. 1-2, pp. 80–84, 2002.
- [43] X. Yang, C. Cao, L. Erickson, K. Hohn, R. Maghirang, and K. Klabunde, “Photo-catalytic degradation of Rhodamine B on C-, S-, N-, and Fe-doped TiO₂ under visible-light irradiation,” *Applied Catalysis B*, vol. 91, no. 3-4, pp. 657–662, 2009.
- [44] W. S. Tung and W. A. Daoud, “New approach toward nanosized ferrous ferric oxide and Fe₃O₄-doped titanium dioxide photocatalysts,” *Applied Materials & Interfaces*, vol. 1, pp. 2453–2461, 2009.
- [45] J. Xu, Y. Ao, and D. Fu, “A novel Ce, C-codoped TiO₂ nanoparticles and its photocatalytic activity under visible light,” *Applied Surface Science*, vol. 256, no. 3, pp. 884–888, 2009.
- [46] H. Žabová and V. Čírkva, “Microwave photocatalysis III. Transition metal ion-doped TiO₂ thin films on mercury electrodeless discharge lamps: preparation, characterization and their effect on the photocatalytic degradation of monochloroacetic acid and Rhodamine B,” *Journal of Chemical Technology and Biotechnology*, vol. 84, no. 11, pp. 1624–1630, 2009.
- [47] M. Subramanian, S. Vijayalakshmi, S. Venkataraj, and R. Jayavel, “Effect of cobalt doping on the structural and optical properties of TiO₂ films prepared by sol-gel process,” *Thin Solid Films*, vol. 516, no. 12, pp. 3776–3782, 2008.
- [48] A. Nishimura, N. Sugiura, S. Kato, N. Maruyama, and S. Kato, “High yield CO₂ conversion into CH₄ by photocatalyst multilayer film,” in *Proceedings of the 2nd International Energy Conversion Engineering Conference*, pp. 824–832, AIAA2004-5619, August 2004.
- [49] A. Nishimura, N. Sugiura, M. Fujita, S. Kato, and S. Kato, “Influence of photocatalyst film forming conditions on CO₂ reforming,” in *Proceedings of the 3rd International Energy Conversion Engineering Conference*, pp. 248–257, AIAA2005-5536, August 2005.
- [50] A. Nishimura, N. Sugiura, M. Fujita, S. Kato, and S. Kato, “Influence of preparation conditions of coated TiO₂ film on CO₂ reforming performance,” *Kagaku Kogaku Ronbunshu*, vol. 33, no. 2, pp. 146–153, 2007.
- [51] A. Nishimura, M. Fujita, S. Kato, and S. Kato, “CO₂ reforming performance of coated TiO₂ film with supported metal,” *Kagaku Kogaku Ronbunshu*, vol. 33, no. 5, pp. 432–438, 2007.
- [52] C. C. Pan and J. C. S. Wu, “Visible-light response Cr-doped TiO₂-xNx photocatalysts,” *Materials Chemistry and Physics*, vol. 100, no. 1, pp. 102–107, 2006.
- [53] S. W. Bae, P. H. Borse, S. J. Hong et al., “Photophysical properties of nanosized metal-doped TiO₂ photocatalyst working under visible light,” *Journal of the Korean Physical Society*, vol. 51, no. 1, pp. S22–S26, 2007.
- [54] M. Anpo, “Photocatalysis on titanium oxide catalysts—approaches in achieving highly efficient reactions and realizing the use of visible light,” *Catalysis Surveys from Japan*, vol. 1, no. 2, pp. 169–179, 1997.
- [55] B. Sun, E. P. Reddy, and P. G. Smirniotis, “Effect of the Cr⁶⁺ concentration in Cr-incorporated TiO₂-loaded MCM-41 catalysts for visible light photocatalysis,” *Applied Catalysis B*, vol. 57, no. 2, pp. 139–149, 2005.
- [56] A. V. Korzhak, N. I. Ermokhina, A. L. Stroyuk et al., “Photocatalytic hydrogen evolution over mesoporous TiO₂/metal nanocomposites,” *Journal of Photochemistry and Photobiology A*, vol. 198, no. 2-3, pp. 126–134, 2008.
- [57] E. A. Streltsov, R. M. Lazorenko-Manevich, V. P. Pakhomov, and A. I. Kulak, “Surface states formed on titanium dioxide by deposition of copper,” *Electrochemistry*, vol. 19, p. 1148, 1983.
- [58] Japan Society of Mechanical Engineering, *Heat Transfer Handbook*, Maruzen, Tokyo, Japan, 1st edition, 1993.
- [59] A. Nishimura, N. Komatsu, G. Mitsui, M. Hirota, and E. Hu, “CO₂ reforming into fuel using TiO₂ photocatalyst and gas separation membrane,” *Catalysis Today*, vol. 148, no. 3-4, pp. 341–349, 2009.
- [60] Y. Nosaka and A. Nosaka, *Introduction of Photocatalyst*, Tokyotosho, Tokyo, Japan, 1st edition, 2004.



The Scientific World Journal

Hindawi Publishing Corporation
<http://www.hindawi.com>

Volume 2013



Hindawi

- ▶ Impact Factor **1.730**
- ▶ **28 Days** Fast Track Peer Review
- ▶ All Subject Areas of Science
- ▶ Submit at <http://www.tswj.com>